

Recent glitches detected in the Crab pulsar

Jingbo Wang^{1,2}

and

Na Wang^{1,3}

and

Hao Tong⁴

and

Jianping Yuan¹

Received _____; accepted _____

¹Xinjiang Astronomical Observatory, Chinese Academy of Science, 40-5 South Beijing Road, Urumqi, Xinjiang, China, 830011

²Graduate School, Chinese Academy of Sciences, Beijing, China, 100049

³Key Laboratory of Radio Astronomy, Chinese Academy of Science, Nanjing, China, 210008; na.wang@uao.ac.cn

⁴Institute of High Energy Physics, Chinese Academy of Sciences, Beijing, China, 100049

ABSTRACT

From 2000 to 2010, monitoring of radio emission from the Crab pulsar at Xinjiang Observatory detected a total of nine glitches. The occurrence of glitches appears to be a random process as described by previous researches. A persistent change in pulse frequency and pulse frequency derivative after each glitch was found. There is no obvious correlation between glitch sizes and the time since last glitch. For these glitches $\Delta\nu_p$ and $\Delta\dot{\nu}_p$ span two orders of magnitude. The pulsar suffered the largest frequency jump ever seen on MJD 53067.1. The size of the glitch is $\sim 6.8 \times 10^{-6}$ Hz, ~ 3.5 times that of the glitch occurred in 1989 glitch, with a very large permanent changes in frequency and pulse frequency derivative and followed by a decay with time constant ~ 21 days. The braking index presents significant changes. We attribute this variation to a varying particle wind strength which may be caused by glitch activities. We discuss the properties of detected glitches in Crab pulsar and compare them with glitches in the Vela pulsar.

Subject headings: pulsars: general pulsars: individual: PSR B0531+21 stars: neutron

1. Introduction

The Crab Nebula is the remnant of supernova explosion recorded by Chinese astronomers in AD 1054. It is the archetype of center-filled supernova remnants (or plerions) with a distant of ~ 2 kpc and one of most well-studied objects in almost all wavebands from low frequency radio to very high energy γ -ray. The overall non-thermal radiation of Crab nebula is mainly dominated by synchrotron process and inverse compton scattering. The synchrotron origin of the optical and radio continuum emission was proposed by Shklovskii (1953) and experimentally confirmed by polarization observations (Dombrovsky 1954).

The nebula is powered by the central Crab pulsar (PSR B0531+21). It is the second brightest pulsar in the northern sky at radio waveband and visible through the whole observable electromagnetic spectrum. In addition, the pulsar is one of the best studied and most energetic pulsar. The spin down power for the pulsar is $\dot{E} = 4.6 \times 10^{38}$ erg s^{-1} . Approximately 10% - 20% of the spin-down energy of the pulsar is converted into the radiation of the nebula. Its pulse frequency ($\nu = 30$ Hz) and pulse frequency derivative ($\dot{\nu} = -3.7 \times 10^{-10}$ s $^{-2}$) yields an characteristic age of 1240 years, very close to the actual age.

The average emission profiles of Crab pulsar are dominated by a main pulse (MP) and an interpulse (IP). The MP and IP are separated ~ 0.4 in pulse phase in all wavelength bands. But the pulse peaks are not fully aligned in phase over the entire energy range. Previous timing of the pulsar over many orders of magnitude of energy found that there is a delay of the radio main pulse compared to the first peak seen from optical to hard γ -rays. Recent measurements of the optical, X, γ -ray to radio lag are: 255 μs (Oosterbroek et al. 2008), 275 μs (S. Molkov et al. 2009), 281 μs (Abdo et al. 2010), respectively. The small differences in pulse phase alignment allow us to study the emission regions at very

small scales. Romani & Yadigaroglu (1995) have proposed that the radio precursor comes at the polar cap, whereas the main pulse and interpulse originate in the outer gap of the magnetosphere, and higher energy pulses are generated at significantly greater heights. Therefore, precise timing of mean pulse profiles over the full range of electromagnetic spectrum is a powerful tool for understanding of the nature and spatial origin of the emission mechanisms.

The Crab Pulsar, just like many young pulsars, is influenced by significant glitches and timing noise in pulse frequency. Timing noise in the Crab pulsar is the dominant component in the timing residuals after removal of the spin-down model and glitch effects from the pulse phase and seen as continuous, noise-like fluctuation in frequency. Scott et al. (2003) shows the timing noise is composed of two components: a long-term quasi-periodic oscillation with a period of 568 ± 10 days and a red noise process with an approximately f^{-3} power density spectrum.

Pulsar glitches are characterized by the sudden increases in pulse frequency. Glitches are rather rare and unpredictable phenomena, and they vary significantly for different pulsars. The characteristics of glitches and the post-glitch recovery behavior provide an important diagnostic tool to study neutron star interiors (e.g., Ruderman 1969; Baym et al. 1969). For the Crab pulsar, twenty four glitches have been detected from 1969 to 2008 (Lyne et al. 1993; Wong et al. 2001; Wang et al. 2001a; Espinoza et al. 2011a). The glitches of Crab pulsar are characterized by their small relative size, rapid exponential relaxation towards extrapolated pre-glitch frequency and a persistent change in frequency derivative at each glitch. Moreover, the large glitches in 1989 and 1996 manifests gradual spin-up right after the initial frequency jump and each glitch may accompanied by an "aftershock" or secondary spin-ups 20-40 days after an event. The persistent increase in the magnitude of pulse frequency derivative may be due either to an increase in the external

torque (Link et al. 1992) or a variation in the momentum of inertia acted on by the torque (Alpar et al. 1996).

In order to study the glitch process, long-term monitoring of frequent glitching pulsars such as Crab and Vela are necessary. Here we present timing observations of the Crab pulsar from 2000 to 2010. Nine glitches have been observed at Xinjiang Astronomical Observatory during this period.

2. Observations and Data Reduction

Timing observations of Crab pulsar at 1540 MHz commenced in 2000 January as part of pulsar monitoring program at Xinjiang Astronomical Observatory (Wang et al. 2001b), with about one observing session per week. A dual-channel room temperature receiver (~ 100 K) was used and then updated to a cryogenic system in 2002 July, which allow us to detect pulsars with a mean flux density greater than 0.5 mJy. The two hands of circular polarization are sent to a filter-bank consisting of 2×128 channels of width 2.5 MHz. The data are 1-bit digitized and sampled at 1-ms intervals. Time is provided by a hydrogen maser calibrated by the Global Position System (GPS) and a latched microsecond counter. The integration time of each observation for the Crab pulsar is 16 minutes.

The offline data was dedispersed to remove the dispersion effects of interstellar medium and folded at nominal topocentric period to produce a mean pulse profile. Topocentric times of arrival (ToAs) were obtained by cross-correlating the mean pulse profile with a noise-free template using PSRCHIVE soft package (Hotan et al. 2004). Local arrival times were converted to Solar-system barycenter times by using TEMPO2¹(Hobbs et al. 2006) with Jet Propulsion Laboratory ephemeris DE405 (Standish 1998). ToAs are weighted by

¹See <http://www.atnf.csiro.au/research/pulsar/tempo2/>.

the inverse square of their uncertainty. Uncertainties in the fitted parameters are taken to be twice the formal uncertainties obtained from TEMPO2.

The pulse phase ϕ predicted by standard timing model is expressed as:

$$\phi(t) = \phi_0 + \nu(t - t_0) + \frac{1}{2}\dot{\nu}(t - t_0)^2 + \frac{1}{6}\ddot{\nu}(t - t_0)^3, \quad (1)$$

where ϕ_0 is the pulse phase at reference time t_0 .

Glitches are usually described as combinations of step changes of ν and $\dot{\nu}$, $\ddot{\nu}$, parts of which decay exponentially:

$$\nu(t) = \nu_0(t) + \Delta\nu_p + \Delta\dot{\nu}_p t + \frac{1}{2}\Delta\ddot{\nu}_p t^2 + \Delta\nu_d e^{-t/\tau_d}, \quad (2)$$

$$\dot{\nu}(t) = \dot{\nu}_0(t) + \Delta\dot{\nu}_p + \Delta\ddot{\nu}_p t + \Delta\dot{\nu}_d e^{-t/\tau_d}, \quad (3)$$

where $\nu_0(t)$ and $\dot{\nu}_0(t)$ are the pulse frequency and pulse frequency derivative extrapolated from pre-glitch model, respectively; $\Delta\nu_p$, $\Delta\dot{\nu}_p$ and $\Delta\ddot{\nu}_p$ are the permanent changes in frequency, its first and second derivatives relative to the extrapolated pre-glitch values, respectively, and $\Delta\nu_d$ is the amplitude of an exponential relaxation component with a decay time constant of τ_d . The total frequency and frequency derivative changes at the time of the glitch are $\Delta\nu_g = \Delta\nu_d + \Delta\nu_p$ and $\Delta\dot{\nu}_g = \Delta\dot{\nu}_d + \Delta\dot{\nu}_p$, respectively. And the degree of recovery can be described by parameter: $Q = \Delta\nu_d/\Delta\nu_g$. The pulsar position used in the reduction is taken from the Jodrell Bank Crab Pulsar Timing Results Monthly Ephemeris²(Lyne et al. 1993).

3. Results

Nine glitches have been observed in the Crab pulsar during the period from 1999 October to 2010 September (MJD 51455 to MJD 55446). However, according to Espinoza

²See <http://www.jb.man.ac.uk/pulsar/crab.html>.

et al.(2011a), there were eleven glitches during the period. We missed two small glitches (5 and 9) because of the observation gaps. Table 1 lists the pre- and post-glitch rotation parameters. Estimated uncertainties in the last quoted digit are given in brackets. As shown in Table 1, several interglitch intervals are very short. It is quite difficult to get the value of $\ddot{\nu}$ for such a short data span. In addition, these $\ddot{\nu}$ values could be affected by the effect of post-glitch exponential decay. Therefore, we keep the $\ddot{\nu}$ at a fixed value which can make the braking index equal to 2.51 for these very short interglitch intervals. The glitch parameters are given in Table 2. The glitch parameters except the glitch epoch were obtained from TEMPO2. The glitch epoches given in the second column of Table 2 which have accuracy of ~ 0.1 day were obtained from the Ephemeris (Lyne et al. 1993). We list the two missed glitches (5 and 9) in Table 2 for completeness with the glitch sizes taken from Espinoza et al.(2011a). Because of the short interglitch intervals and observation gaps, our observations around the epoch of most glitches are not frequent enough to determine the decay timescale. In general, our results are consistent with Espinoza et al. (2011a). Instead of directly fitting glitch parameters in TEMPO2, the glitch parameters given by Espinoza et al. (2011a) were obtained by comparing the timing solutions before and after the glitch.

Table 1: Pre- and post-glitch timing solutions.

Int.	ν (s^{-1})	$\dot{\nu}$ (10^{-9} s^{-2})	$\ddot{\nu}$ (10^{-21} s^{-3})	Epoch (MJD)	MJD Range	No. of ToAs	RmsRes (μs)
–1	29.843629669(3)	–0.3745060(4)	10.8(3)	51622	51547–51738	33	1399
1–2	29.838744465(6)	–0.3744321(79)	11.8	51773	51745–52080	11	803
2–3	29.833181422(14)	–0.3742666(2)	9.4(1)	51945	51824–52080	36	723
3–4	29.827781949(6)	–0.3742107(81)	11.8	52112	52088–52140	10	830
4–5	29.820962244(1)	–0.3798937(1)	10.7(6)	52323	51151–52495	40	987
5–6	29.813984966(4)	–0.3738076(43)	11.7	52539	52503–52574	11	685
6–7	29.803976844(1)	–0.3735181(1)	10.8(3)	52849	52605–53063	63	1085
7–8	29.792879069(4)	–0.3734151(8)	19.9(11)	53193	53133–53253	36	698
8–9	29.789846906(3)	–0.3733023(30)	11.7	53287	53260–53315	8	363
9–10	29.7725067846(7)	–0.37277839(1)	11.45(4)	53825	53685–53965	161	814
10–11	29.752746656(1)	–0.3721811(1)	11.7(6)	54439	54306–54566	95	700
11–	29.7282686152(5)	–0.37141433(4)	11.93(1)	55201	54949–55194	194	1150

The rotation history is presented in Fig.1 and Fig.2. The values of frequency and frequency derivative in the figures were obtained from independent fits to short sections of the data. The uncertainties of frequency and frequency derivative in the plots are 1σ from the TEMPO2 fit. These figures include timing residuals in phase relative to the pre-glitch timing model (panel (a)), variation of frequencies obtained at different epochs relative to the pre-glitch model (panel (b)), and variations of frequency derivatives (panel (c)). These subplots in each figure are arranged in chronological order. We discuss the detailed results of the nine glitches in the following sections.

3.1. The largest glitch

The Crab pulsar suffered its largest frequency jump ($\Delta\nu_g/\nu \sim 2 \times 10^{-7}$) ever seen in 2004 March (MJD 53067.1). The size of the event is more than 3.5 times that of the glitch occurred in 1989. Despite the fraction of increase in frequency is still much smaller than the typical value of the Vela pulsar, the glitch amplitude is comparable to small glitches of the Vela pulsar. Although we could not identify the exponential decay process from Figure 1, we can still obtain the decay time constant and the amplitude of the transient frequency jump with high significance by fitting the two parameters in TEMPO2. The recovery fraction is $\sim 82\%$ and the decay time constant is ~ 21 days which is largest among all the glitches in the Crab pulsar. The glitches occurred in 1969, 1975 and 1989 have a smaller decay time constant than Glitch 7 (Lyne et al. 1993; Wong et al. 2001). As shown in Table 2 and Figure 1, there was a remarkable permanent increase in pulse frequency and the magnitude of the frequency derivative, $\Delta\nu_p \sim 1.2 \times 10^{-6}$ Hz and $\Delta\dot{\nu}_p \sim -202 \times 10^{-15} \text{ s}^{-2}$, respectively. Note that these two parameters are also larger than that of any other glitch in the Crab pulsar.

Table 2: The glitch parameters.

GLT. No.	Glitch Epoch MJD(date)	$\Delta\nu_g$ (10^{-6} s^{-1})	$\Delta\nu_p$ (10^{-6} s^{-1})	$\Delta\dot{\nu}_p$ (10^{-15} s^{-2})	Q	τ_d (d)	MJD Range	RmsRes (μs)
1	51739.4(000714)	—	0.174(32)	-54(10)	—	—	51505–51800	1089
2	51804.9(000917)	—	0.029(21)	-6(10)	—	—	51745–51938	608
3	52083.8(000624)	—	0.409(17)	-79(5)	—	—	51811–52140	792
4	52146.0(010824)	—	0.132(23)	-3(9)	—	—	52088–52301	607
5	52497.3(020812)	0.101(3) ^a	—	—	—	—	—	—
6	52587.1(021109)	—	0.046(23)	-5(8)	—	—	52503–52772	788
7	53067.1(040303)	6.76(13)	1.211(56)	-202(5)	0.82(2)	21.1(8)	52557–53216	1038
8	53254.2(040910)	—	0.090(21)	-17(22)	—	—	53166–53320	598
9	53331.1(041122)	0.08(1) ^a	—	—	—	—	—	—
10	53970.0(060822)	0.41(9)	0.132(6)	-19(1)	0.68(8)	7.3(34)	53712–54142	761
11	54580.0(080423)	—	0.516(89)	-7(6)	—	—	54450–54672	579

^aThe glitch sizes are taken from Espinoza et al. (2011a).

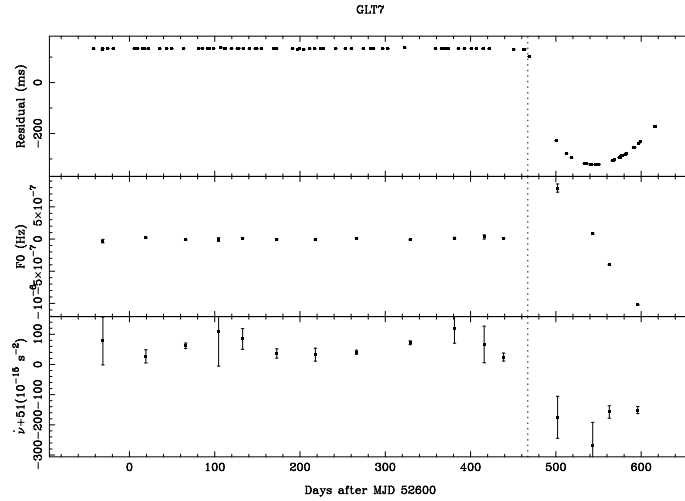


Fig. 1.— The largest glitch (Glitch 7 of this work) : (a) timing residuals relative to the pre-glitch model. (b) variations of the frequency residuals $\Delta\nu$ relative to the pre-glitch solution. (c) the variations of $\dot{\nu}$. The dashed vertical line indicates the epoch of the glitch.

3.2. The other glitches

The frequency jump of Glitch 1 can be easily recognized from the middle panel of GLT1 in Fig.2. The post-glitch increment of pulse frequency derivative can be seen in the bottom panel as well, and this glitch caused a permanent change of pulse frequency derivative. Glitch 2 is a much smaller event and only a little frequency jump could be seen in GLT2 of Fig.2. As shown in Table 2, no evident $\Delta\nu_p$ is measured. The subplot GLT3 in Fig.2 is very similar to that of GLT1. However, the amplitude of $\Delta\nu_p$ and $\Delta\dot{\nu}_p$ are larger than GLT1. Glitch 4 is another small glitch. Compared with the pre-glitch solution, we can see the pulse frequency after the glitch decreased gradually from the frequency residuals plot of Glitch 4. But the pulse frequency derivative of Glitch 4 almost remain the same for about 100 days after the glitch and decreased then. And Glitch 6 is a small glitch as well. The timing and frequency residuals plots of Glitch 6 look similar to that of Glitch 4. The pulse frequency derivative after the glitch exhibit a small fluctuation and no obvious $\Delta\dot{\nu}_p$ is detected as well. Apparently, as seen from GLT8 of Figure 2, we miss the frequency jump of Glitch 8 because of the observation gap. However, as shown in Table 2, we got a significant value for $\Delta\nu_p$ and the $\Delta\dot{\nu}_p$ induced by the glitch can be identified from the bottom panel of GLT8. Glitch 10 is a relative large one in magnitude with a small recovery fraction $\sim 68\%$ and a short decay time constant . The exponential fit for the glitch in 1996 (Wong et al. 1996) has nearly the same recovery fraction, but the measured $\Delta\nu_p$, $\Delta\dot{\nu}_p$, and decay time constant of Glitch 10 are much smaller than that of the glitch in 1996. The last glitch of this paper occurred on MJD 54580.0 with a $\Delta\nu_p$ value similar to Glitch 6. In contrast to pre-glitch timing model, The post frequency residuals decreased steady which indicate a change in the pulse frequency derivative and this could be also seen in the lower panel of GLT11 in Fig.2.

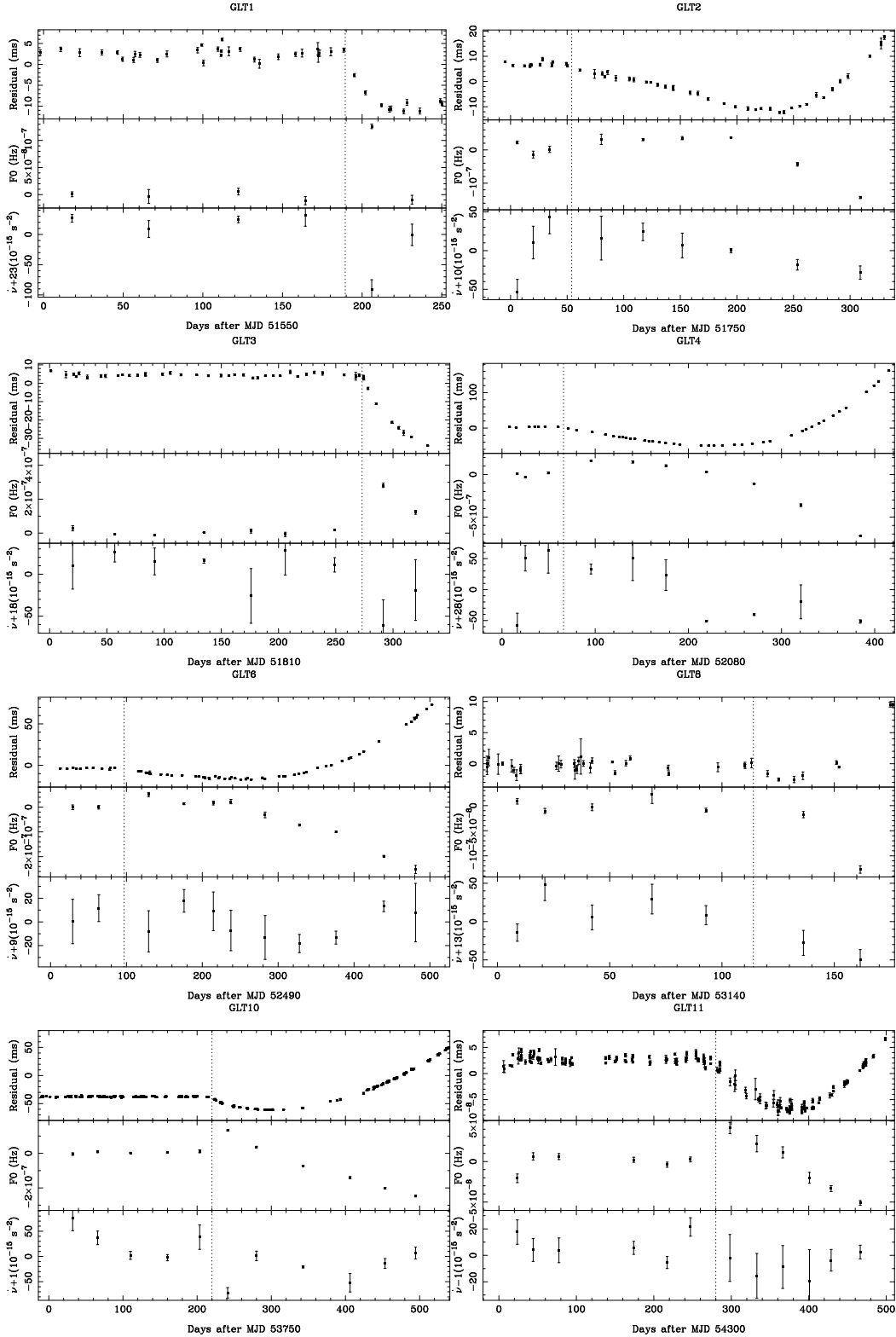


Fig. 2.— Eight glitches (Glitch 1, 2, 3, 4, 6, 8, 10 and 11 of this work) : (a) timing residuals relative to the pre-glitch model. (b) variations of the frequency residuals $\Delta\nu$ relative to the pre-glitch solution. (c) the variations of $\dot{\nu}$. The dashed vertical line indicates the epoch of the glitch.

4. Discussion

4.1. The interglitch intervals

Wong et al. (2001) pointed out that the Crab pulsar glitches appear to be independent events spaced randomly in time. However there were only eight glitches and seven interglitch interval by the time of their work. Therefore, we add the eleven new glitches to the sample for the statistics, which consists a total sample of 19 glitches.

The left panel of Fig.3 shows the observed distribution of interglitch intervals of Crab pulsar from 1983 to 2008. The dashed line represents expected distribution for a Poisson process with average interval λ ,

$$P(T) = 1 - e^{-t/\lambda}, \quad (4)$$

where λ is the mean interglitch interval. The plot shows that for the Crab pulsar the occurrence times of the glitches is well described by Poisson distribution. Fitting of the data gives a mean interglitch interval of 419 days which is significantly smaller than the previous result of 684 days given by Wong et al. (2001), the frequent glitches in recent years mainly contribute to the shorter interval. The standard deviation of the interglitch interval is quite large, 365 days. A Kolmogorov-Smirnov (K-S) test obtained a probability $P_{K-S} = 0.991$, This means that the distribution of interglitch interval agrees well with a Poisson model. Melatos et al. (2008) also found that the occurrence times of the glitches are consistent with Poisson statistics in the Crab and several other glitching pulsars.

By comparison, we present the interglitch intervals of the Vela pulsar and Poisson distribution in the right panel of Fig.3. In total 16 glitches from 1969 to 2006 are included (Cordes et al. 1988, McCulloch et al. 1987, McCulloch et al. 1990, Flanagan 1991, Flanagan 1994a, Flanagan 1994b, Wang et al. 2000, Dodson et al. 2002, Dodson et al. 2004, Lanagan & Buchner 2006). This reveals a mean glitch interval of 912 days. Fig.3 clearly shows

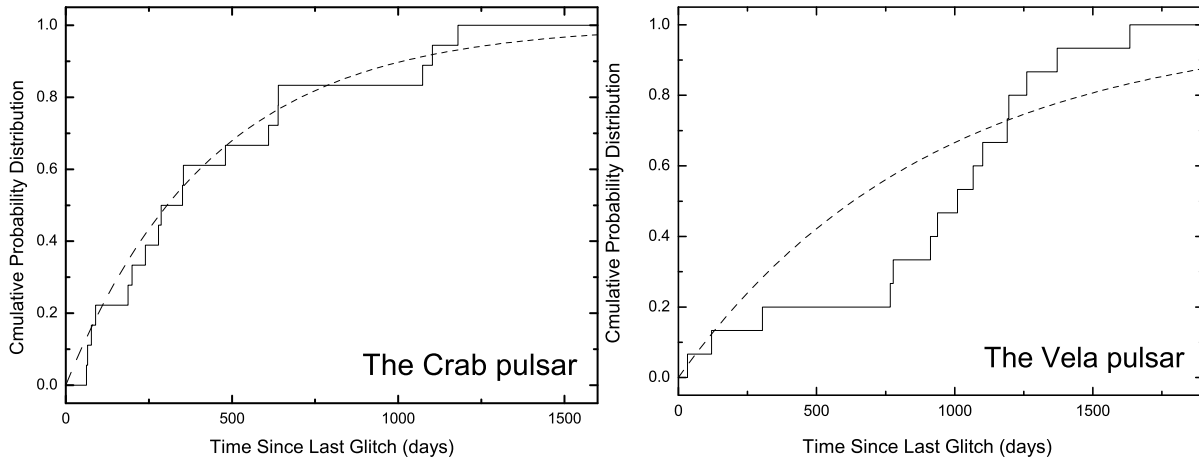


Fig. 3.— Cumulative distribution of interglitch intervals for the Crab (left) and the Vela (right) pulsar. The dashed curves represent a Poisson distribution with a mean interval of 419 and 912 days for them, respectively.

that the distribution of interglitch interval is essentially different from a Poisson prediction for the Vela pulsar. A K-S test with $\lambda = 912$ days shows that we can reject the Poisson model at a 93.9% confidence level. Melatos et al. (2008) shows the glitch occurrence is quasi-periodic. The typical and relatively quasi-periodic glitch occurrence present in each pulsar might indicate that a critical lag between the rotation of the superfluid and crust has to be achieved in order for a glitch to occur (Alpar et al. 1993). Figure 4 shows the relation between the fractional glitch size and the time since previous glitch for the Crab and the Vela pulsars. The size of glitches for the Crab pulsar are obtained from Espinoza et al. (2011a) and this work. The Crab pulsar has a wide range in both parameters while most glitches of Vela pulsar are large and have longer interglitch intervals. For both pulsars, little correlation are found between glitch sizes and the time since last glitch, even though theoretical predictions prefer that the amplitude of a glitch would be proportional to the intervals of preceding glitch (e.g., Alpar et al. 1989; Ruderman et al. 1998).

4.2. Properties of observed glitches

Some pulsars like the Crab only experienced small glitches (e.g., Yuan et al. 2010; Krawczyk et al. 2003), while Vela-like pulsars are characterized by large size glitches (e.g., Shemar & Lyne 1996; Wang et al. 2000). Some pulsars exhibit wide glitch size distribution spanning three or even four orders of magnitude (10^{-10} to 10^{-6} Hz; e.g., Lyne 1987; Janssen & Stappers 2006). The absence of large glitch in the Crab pulsar is likely attributed to its relative young age; the stresses build up during steady spin down can partly relieved by gradual process such as vortex creep and plastic flow at high crustal temperature (e.g., Ruderman 1991; McKenna & Lyne 1990). As shown in Figure 4, there is no significant correlation between the glitch size and the time since last glitch for the Crab and Vela pulsars. In addition, lack of correlation between glitch size and preceding interglitch interval in most pulsars (e.g., Yuan et al. 2010; Wang et al. 2010) suggests that the triggering of glitches is not closely related to global slowdown of the pulsar.

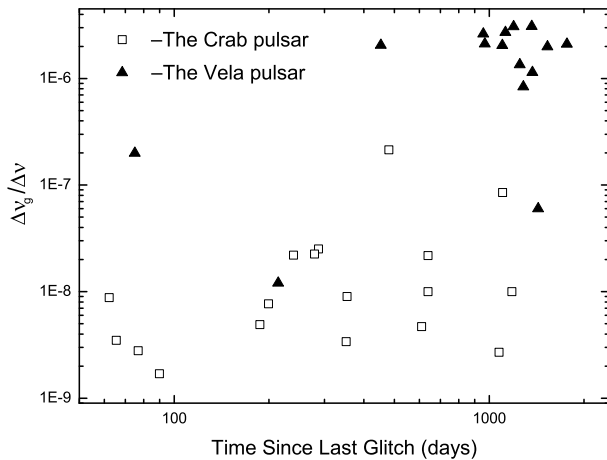


Fig. 4.— Glitch size against the time since the previous glitch since 1989 (earlier glitches have been omitted as a result of possible gaps in the timing record). Squares and filled triangles indicate the Crab and the Vela pulsars glitches, respectively.

The activity parameter $A_g \equiv (\Sigma \Delta \nu_p) / t_{obs}$ is defined to be a long-term indicator of

glitch effects (Wong et al. 2001). Figure 5 shows a cumulative plot of persistent changes in ν as a function of time for the Crab pulsar since 1969. The activity parameter A_g , which is represented by the slope of this relation, is about $1.4 \times 10^{-5} |\dot{\nu}|$. This value is essentially the same as that of given by Wong et al. (2001). It implies that the rate of angular momentum loss caused by glitch has not changed significantly, in spite of high glitch rate during the past 10 yr. The persistent changes in $\dot{\nu}$ caused by the Crab pulsar glitches is probably due

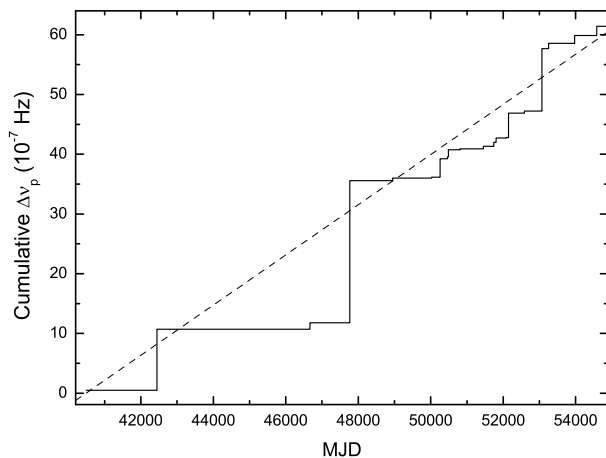


Fig. 5.— Cumulative $\Delta\nu_p$ caused by glitches plotted as a function of time based on data from Table 2. The dashed line represent a least-squares fit to the midpoints of the frequency jumps . The slope of the dashed line is an estimate of the activity parameter A_g .

to the formation of new vortex capacitors (Alpar et al. 1996). Superfluid decouples from the steady slow down of star crust leading to the decrease of moment of inertia. Therefore, the external torque acts on a lower moment of inertia and thus $|\dot{\nu}|$ increases. On the other hand, the variation of external torque result in change in $\dot{\nu}$, maybe due to an increase in the dipole magnetic field (Ruderman et al. 1998) or a change angle between magnetic and rotation axis (Link et al. 1998). A long term asymptotic exponential rise in frequency, as shown in Figure 7b of Lyne et al. (1993) was observed after the 1975, 1981, 1986 and 1989 glitches. However, no similar event has been observed since. This is probably because

the timescale of asymptotic rise exceeds the interglitch intervals. The wide range of glitch parameters implies a local phenomenon of the Crab pulsar in which starquakes could be responsible for Crab glitches. The small size of glitches, permanent postglitch offsets in the frequency derivative and the large recovery fraction of Crab pulsar glitches shown by our and previous results are all consistent with starquakes model (e.g., Lyne 1992; Alpar et al. 1994, 1996; Link et al. 1998; Franco et al. 2000; Crawford and Demianski 2003). By contrast, starquakes can not be the cause of glitches for the Vela pulsar (Lyne 1992; Alpar et al. 1993; Chau et al. 1993; Alpar et al. 1995; Crawford and Demianski 2003).

4.3. The braking index

The high glitch rate makes it difficult to measure the braking index of the Crab pulsar. The interval between Glitch 9 and Glitch 10 is relatively longer. And the Crab pulsar has not experienced any glitch after 2008 April (Glitch 11). We measure the braking indices for these two data spans. Observed values of frequency and its first and second derivatives can be used to obtain the braking index n , using the equation:

$$n = \nu \ddot{\nu} / \dot{\nu}^2. \quad (5)$$

In order to avoid the effect of exponential decay of the steps in $\dot{\nu}$ and $\ddot{\nu}$ of the glitch, we omitted the observations about one year after the previous glitch. The braking indices are calculated based on the timing parameters listed in Table 1 for these two data spans, giving values of 2.454(7) and 2.571(3), respectively. The previous measured value of braking index show a remarkable constant value 2.51 (Lyne et al. 1993, Wong et al. 2001). It is clear that there is an evident change in braking index. The $\Delta\ddot{\nu}$ changes have been found by Wong et al. (2001). In fact, the changes in braking index which have become more marked during the last 20 years or so, when the amount of glitch activity increased. The value of braking index after Glitch 11 is larger than the previous measured value, whereas the other braking

index measured between Glitch 9 to Glitch 10 is much smaller. So the scatter of braking index is much larger than that given by Lyne et al. (1993) and Wong et al. (2001).

The reason of a varying braking index may be due to a varying particle wind. A particle wind in addition to the magnetic dipole radiation may account for a braking index less than three (Michel 1969; Manchester et al. 1985; Xu & Qiao 2001; Espinoza et al. 2011b). The existence of particle wind is verified by observations of intermittent pulsars (Kramer et al. 2006; Camilo et al. 2011). A fluctuating wind may contribute to the long term timing noise (Lyne et al. 2010; Liu et al. 2011). Another consequence of a varying particle wind will be a varying braking index. This may be the case of PSR J1846-0258 (Livingstone et al. 2011). In this paper, we apply the pulsar wind model of Xu & Qiao (2001) to the Crab pulsar. (Other pulsar wind models are similar. They contain a dipole component and wind component, e.g. Spitkovsky 2006.) Employing the polar cap model of Ruderman & Sutherland (1975) and considering that the wind strength may depart from the long term average value, Figure 6 shows the braking index as a function of wind strength (Xu & Qiao 2001)³. A larger wind strength will cause the braking index smaller. A wind strength of 1.19 will give a braking index 2.45, and a wind strength of 0.87 corresponds to a braking index of 2.57. Therefore, a varying wind strength will result in a varying braking index naturally. The variations from long term average value are mainly fluctuations. This fluctuations may be caused by frequent glitches of the Crab pulsar, similar to the glitch induced magnetospheric activities seen in magnetars (Kaspi et al. 2003).

Since we only have two braking index measurements at present, an estimation of possible short term net increase in wind strength is very uncertain. Based on these two

³For discussions of different particle acceleration models see Xu & Qiao (2001). The corresponding calculations will only differ quantitatively when employing different particle acceleration models.

measurements, the net increase in wind strength is three percent. The corresponding relative change in slow-down rate is 0.007. Accurate to one order of magnitude, this is consistent with the largest increase in slow-down rate after glitches as shown in Table 3.

5. Summary

We have presented timing observations of the Crab pulsar from 2000 to 2010. During this period, this pulsar manifest a higher rate of glitch activities than previous, with nine glitches detected over a period of 8 yr. The number of glitches in the Crab pulsar has increased considerably. The distribution of interglitch intervals is still in agreement with a random process. There is no correlation between the glitch amplitude and the time since the last glitch. In accord with previous study (Lyne et al. 1993, Wong et al. 2001), permanent changes in pulse frequency derivative are observed at the time of each glitch. Since the relative small permanent frequency changes for the recent glitches, the average pulse frequency derivative caused by glitches (represent by the activity parameter A_g) almost remains the same, in spite of the high glitching rate. The braking index shows an relative obvious variation, which may be due to a varying particle wind strength induced by glitches.

6. Acknowledgments

This work is supported by NSFC project 10673021, the Knowledge Innovation Program of the Chinese Academy of Sciences, Grant No. KJCX2-YW-T09, National Basic Research Program of China (973 Program 2009CB824800) and West Light Foundation of CAS (No. XBBS201021).

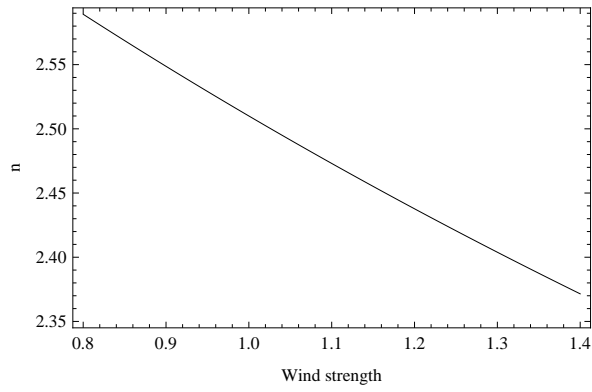


Fig. 6.— The braking index as a function of wind strength. Calculations for the Crab pulsar. Wind strength 1 is the long term average value, which corresponds to a braking index of 2.51 (Xu & Qiao 2001). Wind strength 1.2 means the wind luminosity is 1.2 times the long term average value, etc.

REFERENCES

- Alpar M. A., Cheng K. S., Pines D., 1989, *ApJ*, 346, 823
- Alpar M. A., Kiziloglu U., van Paradijs J., eds, 1995, *The Lives of the Neutron Stars*
- Anderson S. B., Cordova F. A., Pavlov G. G., Robinson C. R., Thompson R. J., 1993, *ApJ*, 414, 867
- Baym G., Pethick C., Pines D., 1969, *Nature*, 224, 673
- Boynton P. E., Groth E. J., Hutchinson D. P., Nanos G. P., Partridge R. B., Wilkinson D. T., 1972, *ApJ*, 175, 217
- Camilo F., Ransom S. M., Chatterjee S., Johnston S., Demorest P., 2011, *ArXiv e-prints*
- Cordes J. M., 1980, *ApJ*, 237, 216
- Cordes J. M., Downs G. S., Krause-Polstorff J., 1988, *ApJ*, 330, 847
- Crawford F., Demiański M., 2003, *ApJ*, 595, 1052
- Dodson R. G., McCulloch P. M., Lewis D. R., 2002, *ApJ*, 564, L85
- Espinoza C. M., Lyne A. G., Stappers B. W., Kramer M., 2011a, *MNRAS*, 414, 1679
- Espinoza C. M., Lyne A. G., Kramer M., Manchester R. N., Kaspi V. M., 2011b, *ApJ*, 741, L13
- Flanagan C., 1991, *IAU Circ.*, 5311, 3
- Flanagan C., McCulloch P. M., 1994, *IAU Circ.*, 6038, 2
- Flanagan C. S., Buchner S. J., 2006, *Central Bureau Electronic Telegrams*, 595, 1
- Franco L. M., Link B., Epstein R. I., 2000, *ApJ*, 543, 987

- Groth E. J., 1975, *ApJS*, 29, 431
- Hobbs G. B., Edwards R. T., Manchester R. N., 2006, *MNRAS*, 369, 655
- Hotan A. W., van Straten W., Manchester R. N., 2004, *PASA*, 21, 302
- Kaspi V. M., Gavriil F. P., 2003, *ApJ*, 596, L71
- Kramer M., Lyne A. G., O'Brien J. T., Jordan C. A., Lorimer D. R., 2006, *Science*, 312, 549
- Krawczyk A., Lyne A. G., Gil J. A., Joshi B. C., 2003, *MNRAS*, 340, 1087
- Link B., Epstein R., Baym G., 1992, *ApJ*, 390, L21
- Link B., Franco L. M., Epstein R. I., 1998, *ApJ*, 508, 838
- Liu X.-W., Na X.-S., Xu R.-X., Qiao G.-J., 2011, *Chinese Physics Letters*, 28, 019701
- Livingstone M. A., Ng C.-Y., Kaspi V. M., Gavriil F. P., Gotthelf E. V., 2011, *ApJ*, 730, 66
- Lyne A., Hobbs G., Kramer M., Stairs I., Stappers B., 2010, *Science*, 329, 408
- Lyne A. G., 1987, *Nature*, 326, 569
- Lyne A. G., Pritchard R. S., Graham-Smith F., Camilo F., 1996, *Nature*, 381, 497
- Lyne A. G., Pritchard R. S., Smith F. G., 1988, *MNRAS*, 233, 667
- Lyne A. G., Pritchard R. S., Smith F. G., 1993, *MNRAS*, 265, 1003
- Lyne A. G., Shemar S. L., Smith F. G., 2000, *MNRAS*, 315, 534
- Lyne A. G., Smith F. G., Pritchard R. S., 1992, *Nature*, 359, 706
- McCulloch P. M., Klekociuk A. R., Hamilton P. A., Royle G. W. R., 1987, *Australian Journal of Physics*, 40, 725

- Manchester R. N., Newton L. M., Durdin J. M., 1985, *Nature*, 313, 374
- Marshall F. E., Gotthelf E., Middleditch J., 2010, American Astronomical Society Meeting, 42, 453
- McCulloch P. M., Hamilton P. A., McConnell D., King E. A., 1990, *Nature*, 346, 822
- McKenna J., Lyne A. G., 1990, *Nature*, 343, 349
- Michel F. C., 1969, *ApJ*, 158, 727
- Middleditch J., Marshall F. E., Wang Q. D., Gotthelf E. V., Zhang W., 2006, *ApJ*, 652, 1531
- Ruderman M., 1969, *Nature*, 223, 597
- Ruderman M., 1991, *ApJ*, 382, 576
- Ruderman M., Zhu T., Chen K., 1998, *ApJ*, 492, 267
- Ruderman M. A., Sutherland P. G., 1975, *ApJ*, 196, 51
- Scott D. M., Finger M. H., Wilson C. A., 2003, *MNRAS*, 344, 412
- Shemar S. L., Lyne A. G., 1996, *MNRAS*, 282, 677
- Spitkovsky A., 2006, *ApJ*, 648, L51
- Standish E. M., 1998, *A&A*, 336, 381
- Wang N., Manchester R. N., Pace R., Bailes M., Kaspi V. M., Stappers B. W., Lyne A. G., 2000, *MNRAS*, 317, 843
- Wang N., Wu X. J., Manchester R., Zhang J., Lyne A. G., Yusup A., 2001a, *Chin. J. Astron. Astrophys.*, 1, 195

Wang N., Manchester R. N., Zhang J., Wu X. J., Yusup A., Lyne A. G., Cheng K. S., Chen M. Z., 2001b, MNRAS, 328, 855

Wong T., Backer D. C., Lyne A., 2001, ApJ, 548, 447

Xu R. X., Qiao G. J., 2001, ApJ, 561, L85

Yuan J. P., Wang N., Manchester R. N., Liu Z. Y., 2010, MNRAS, 404, 289

Zou W. Z., Wang N., Manchester R. N., Urama J. O., Hobbs G., Liu Z. Y., Yuan J. P., 2008, MNRAS, 384, 1063